®2016

Kevin Coffey

All Rights Reserved

Both the direct (Drd1) and indirect (Drd2) pathways contain type IIb neurons whose firing rates are related to stimulation of individual body parts

By

Kevin R. Coffey

A dissertation submitted to the

Graduate School-New Brunswick

Rutgers, the State University of New Jersey

In partial fulfillment of the requirements

For the degree of

Doctor of Philosophy

Graduate Program in Psychology

Written under the direction of

Mark O. West

And approved by

_____

_____

_____

_____

New Brunswick, New Jersey

October, 2016

ABSTRACT OF THE DISSERTATION

Both the direct (Drd1) and indirect (Drd2) pathways contain type IIb neurons whose firing rates are related to stimulation of individual body parts

By Kevin R. Coffey

Dissertation Director:
Mark O. West

The dorsolateral striatum (DLS) is a prominent target of research on control of voluntary movement and sensorimotor integration. The DLS is comprised mainly (95%) of medium spiny projection neurons that receive direct monosynaptic projections from primary somatosensory (S1) and motor (M1) cortices. Roughly 50% of these neurons are type IIb GABAergic, medium spiny projection neurons (MSNs) whose firing rates (FRs) are related to sensorimotor activity of individual body parts. There is also a hypothesized dual organization of DLS outputs known as the "direct and indirect pathways". According to this model, direct pathway MSNs project to the substantia nigra pars reticulata (SNr) and the internal segment of the globus pallidus (GPi), leading to disinhibition of the thalamus and facilitation of movement. Conversely the indirect pathway projects to the SNr via the globus pallidus external segment (GPe) and then the subthalamic nucleus (STN), inhibiting the thalamus and reducing movement. In addition to their distinct projections, MSNs of the direct and indirect pathway are characterized by differential expression of dopamine receptors. Dopamine Drd1 is expressed by direct pathway MSNs, whereas Drd2 is expressed by indirect pathway MSNs. While there has been a significant amount of research testing the functional hypotheses generated by

the direct and indirect pathways framework, no study has attempted to reconcile the very well classified striatal type IIb neurons with the aforementioned functional tenet of the hypothesis. The present study utilized AAV-EF1a-FLEx-Chronos-GFP to visualize and optogenetically identify Drd1 and Drd2 MSNs in Cre-animals. We then performed somatosensory motor exams in order to identify type IIb MSNs and fill the gap in the literature. We found that in Drd1-Cre animals, Chronos-GFP expressing neurons projected to GPi, while in Drd2-Cre animals, Chronos-GFP expressing neurons projected to GPe, providing evidence that Drd1-Cre and Drd2-Cre animals are valid models of the direct and indirect pathways. Further, we were able to unambiguously identify Drd1 and Drd2 MSNs in the striatum of awake, behaving mice using light stimulation. We were subsequently able show that both the direct (Drd1) and indirect (Drd2) pathways contain type IIb neurons with firing related to stimulation of body parts. This evidence brings into question the notion that Drd1 neurons promote movement, while Drd2 neurons inhibit it. Rather, it seems that Drd1 and Drd2 neurons process sensorimotor information similarly, with both Drd1 and Drd2 neurons exhibiting increased phasic firing during body part stimulation and movement. While the anatomical aspects of the direct and indirect pathways hypothesis are strongly corroborated, the functional aspect appears to need a critical reevaluation.

Table of Contents

List of Illustrations & Tables

Introduction

The dorsolateral or sensorimotor striatum (DLS) (Flaherty and Graybiel, 1994) is a prominent target of research on control of voluntary movement, sensorimotor integration, and neuroplasticity involved in procedural learning and habit formation. Dysfunction of the dorsolateral striatum is also heavily researched in Tourette syndrome, obsessive compulsive disorder, psychomotor stimulant addiction, Parkinson's disease, and Huntington's disease. As with all brain areas the DLS does not operate in isolation, and its role in these processes is enlightened by a strong understanding of its chemical and anatomical organization. This understanding of anatomical and chemical organization provides a solid framework for researchers to determine striatum's functional organization, and ultimately to understand precisely how the DLS contributes to normal and abnormal behaviors.

The DLS is comprised mainly (95%) of medium spiny projection neurons (Wilson and Groves, 1980; Kimura et al., 1990). Seminal neuroanatomical studies using tract tracing tools showed that these neurons receive direct monosynaptic projections from primary somatosensory (S1) and motor (M1) cortices in the monkey (Kunzle, 1975; 1977). This work was followed up by studies showing similar anatomical projections which indicated a sensorimotor sector in the rat DLS (Cospito and Kultas-Ilinski, 1981; McGeorge and Faull, 1989). Finally, anatomical studies in mice have also demonstrated corticostriatal terminal distributions similar to those in rats (White and DeAmicis, 1977; Jinno and Kosaka, 2004; Hattox and Nelson, 2007; Tai and Kromer, 2014). S1 and M1 excitatory projections to the DLS converge with nigrostriatal dopaminergic terminals

onto MSNs (Freund et al., 1984).

These anatomical findings played a pivotal role in informing subsequent studies which clarified striatal function. For example, the findings were soon corroborated by physiological studies that revealed clusters of medium spiny neurons (MSNs) whose firing rate (FR) is related to sensorimotor activity of individual body parts (Liles, 1979; Crutcher and DeLong, 1984; Alexander and DeLong, 1985; Lyles and Updyke, 1985) and which project into pallidothalamocortical reentrant loops (Alexander et al., 1986). Thus, the functional organization of the sensorimotor striatum became known as a patchy somatotopy (Flaherty and Graybiel, 1993). A sequence similar to these studies in monkeys soon followed in rats. Anatomical projections indicating a sensorimotor sector in the DLS (Cospito and Kultas-Ilinski, 1981; McGeorge and Faull, 1989) were corroborated by physiological studies demonstrating a patchy somatotopic functional organization in rats similar to that in primates (West et al., 1990; Carelli and West, 1991; Cho and West, 1997).

DLS neurons related to individual body parts are valuable in electrophysiological studies because identification using their characteristic waveform and firing properties enables interpretations that incorporate a remarkable degree of knowledge, considering that the preparation is an awake behaving animal. Specifically, these neurons are type IIb GABAergic, medium spiny projection neurons (Kimura et al., 1990) that receive convergent glutamatergic input from S1 and M1 and dopaminergic input from substantia nigra. The information inherent in recording from these particular DLS neurons makes them well suited for studying key issues such as how they correlate with

movement parameters, the mechanisms affected in parkinsonian models, learning-related corticostriatal plasticity, etc. Moreover, given that one-third to one-half of the DLS population exhibit no discernable relation to somatosensory or motor activity, type IIb neurons appear to constitute an important pool of neurons to study with regard to the sensorimotor integrative functions attributed to the striatum.

To date, few electrophysiological studies in mice have attempted to provide the critical corroboration of sensorimotor properties of DLS neurons (Reig and Silberberg, 2014), perhaps because of the difficulty in manipulating individual body parts in freely moving mice (Coffey et al., 2016). However, mice are becoming an increasingly popular pre-clinical model for studying striatal function because of the access they provide to genetic neuroscience toolkits. Thus, it is imperative that DLS neurons be explored in the mouse model.

In parallel with the discoveries regarding DLS inputs, a series of anatomical studies have been building toward a specialized theory of medium spiny neuron output. The now canonical theory is known as the “direct and indirect pathways” hypothesis, and it originated in seminal papers that hypothesized a dual organization of striatal outputs (Albin and Young, 1989; Alexander and Crutcher, 1990). According to this model, cortical activation produces a release of glutamate that excites direct pathway MSNs projecting to the substantia nigra pars reticulata (SNr) and the internal segment of the globus pallidus (GPi). MSNs are GABAergic and thus inhibit neurons of the GPi and SNr which are also primarily GABAergic projection neurons. This inhibition of GPi and SNr leads to disinhibition of the thalamic glutamatergic neurons, which project to the

cortex and facilitate movement. Conversely the “indirect pathway” is named for projecting indirectly to the SNr via the globus external segment (GPe) and then the subthalamic nucleus (STN). Activation of indirect pathway MSNs inhibits the GABAergic neurons of the GPe, leading to a disinhibition of the glutamatergic neurons of the STN. In turn, the increased activity of excitatory STN neurons activates the SNr GABAergic neurons projecting to the thalamus. Ultimately, this effect is hypothesized to result in the reduction of movement.

In addition to their distinct projections, MSNs of the direct and indirect pathways are characterized by the differential expression of dopamine (DA) receptors. Dopamine Drd1 receptors are hypothesized to be expressed by direct pathway MSNs, whereas dopamine Drd2 receptors are expressed by indirect pathway MSNs (Gerfen et al., 1990). These two receptors are associated with distinct G proteins that are linked to different intracellular signaling pathways and lead to different biochemical responses following DA receptor activation (Frederick et al., 2015). This neurochemical segregation is thought to contribute to the dichotomous effect of the activation of the direct and indirect pathways (Kravitz et al., 2010).

In the years since its inception, the direct and indirect pathways hypothesis has been further refined with regard to chemical and anatomical connectivity, as well as its functional implications for normal and abnormal behavior. One of the central tenets of the hypothesis is the segregation of Drd1 and Drd2 MSNs and their output pathways. However, single-cell labeling studies in rats and monkeys have revealed the existence of striatal projection neurons with highly collateralized axons that provide branches to two

or three of the striatal output structures (Parent et al., 1995; Wu et al., 2000; Levesque and Parent, 2005). Furthermore, there is significant evidence that some striatal MSNs express both Drd1 and Drd2. Estimates from pharmacological manipulations show almost 100% overlap (Aizman et al., 2000), but pharmacological agents are known to have overlapping affinity for Drd1 and Drd2 and more advanced genetic techniques suggest the overlap is minimal (5-6%; Bertran-Gonzalez et al., 2008; Frederick et al., 2015). These studies at least suggest that there is not perfect segregation of the striatal output pathways, or even perfect segregation of Drd1 and Drd2 expression in striatal MSNs. There is even some evidence that these Drd1 and Drd2 co-expressing neurons actually form a novel and pharmacologically distinct receptor complex, the dopamine D1–D2 receptor, which could be evidence for a third output pathway in the basal ganglia (Perreault et al., 2011).

An important advancement in the study of the direct and indirect pathways has been the development of the Cre-recombinase driver mouse using bacterial artificial chromosome constructs (Gong et al., 2007; Gerfen et al., 2013). These mice allow for almost any genetic payload to be delivered to any genetically definable neuronal population through the Cre-LoxP recombinase system. This system is highly flexible and can deliver adeno-viruses which code for proteins such as fluorophores, neural activity indicators, and neural activity manipulators. Most relevant to the study of the direct and indirect pathways are Drd1-Cre and Drd2-Cre mice. Using these animals, researchers are able to further probe the anatomical and functional differences between direct and indirect pathway MSNs. For example, researchers have shown that Drd1 and Drd2

expressing DLS MSNs both receive the vast majority of their cortical input from somatosensory and motor areas (Wall et al., 2013). These animals have also allowed for genetically defined visualization and manipulation of a large number of MSNs simultaneously in either the direct or indirect output pathway. While MSNs are known to collateralize in multiple output nuclei (Parent et al., 1995) and manipulation of Drd2 MSNS can even cause further bridging of the pathways to occur (Cazorla et al., 2014), Cre-driver mice allow for visualization of the entire striatal Drd1 and Drd2 output pathways. Using these mice, researchers have shown repeatedly that striatal Drd1 MSNs in mice primarily project to the GPi and SNr, while Drd2 MSNs primarily project to GPe (Gerfen et al., 2008, Cui et al., 2013; Wall et al., 2013; Kravitz et al., 2010; Cazorla et al., 2014). These animals finally validated a decades old hypothesis which for years had rested on fairly weak support.

Drd1-Cre and Drd2-Cre animals have also allowed researchers to test the primary functional tenet of the direct and indirect pathway hypothesis: that Drd1 MSN activation excites movement, while Drd2 MSN activation inhibits movement (Gerfen et al., 1990). This functional aspect of the direct and indirect pathways hypothesis has been tested by manipulating the pathways and observing behavior, as well as by manipulating behavior and monitoring neural activity in the pathways. By expressing Channel Rhodopsin (ChR2) in the striatum of Drd1-Cre and Drd2-Cre mice, researchers can activate Drd1 or Drd2 MSNs with high selectivity and fine temporal resolution while observing locomotor behavior. In the first study showing direct experimental support for the model, when Drd1 MSN output was increased with light stimulation, mice

increased locomotor behavior, whereas when Drd2 MSN output was increased, mice decreased locomotor behavior and began to freeze (Kravitz et al., 2010). This study indiscriminately activated all striatal Drd1 or Drd2 MSNs, without regard for body part representation in those neurons. It is not clear how activating multiple neurons, each of which could represent any body part (e.g. jaw or whisker), would result in a specific coordinated activity like locomotion, although indiscriminate inhibition might conceivably lead to the freezing behavior observed. Subsequently, researchers monitored the activity of Drd1 and Drd2 MSNs in the dorsolateral striatum using a genetically encoded fluorescent calcium indicator (GECI) GCaMP3 during a behavior that required more specific body part movement. It was shown that activity in both Drd1 and Drd2 MSNs increases during body movement to the left or right (Cui et al., 2013). These results are in direct opposition to the direct and indirect pathways hypothesis, in that Drd2 MSNs should not be more active during movement if they are a global no-go signal. However, that study measured calcium activity in neurons, not necessarily action potentials or the output of the neurons. It also did not account for body part specificity of MSNs in the striatum; instead all Drd1 and Drd2 MSNs were recorded during the movement, without regard for whether their related body parts were moving or not.

Since the study by Cui et al. (2013), several attempts have been made to revamp the direct and indirect pathways functional hypothesis so that Drd1 and Drd2 MSNs may be active together in order to perform specific actions (Friend and Kravitz, 2014). The authors suggest that while Drd1 MSNs are active to select or produce an action such as locomotion, Drd2 MSNs must be active to suppress competing actions such as

grooming. This could ostensibly account for the observed co-activation of pathways during movement, while retaining one of the central functional tenets of the hypothesis intact: that Drd2 MSN activity inhibits movement. Although this is an interesting idea, there is little empirical evidence to support it. Another more recent study attempted to rectify its conflicting evidence with the hypothesis's explanation of parkinsonian symptoms and emphasized the importance of presynaptic as well as somatodendritic Drd2 (Lemos et al., 2016).

Some unresolved issues related to striatal function and signaling in direct and indirect pathways could be informed by studying type IIb neurons in awake behaving mice. As an initial step, we recently demonstrated for the first time that body parts are represented in single unit activity recorded from the DLS in freely moving mice (Coffey et al., 2016). However, while there has been a significant amount of research testing the functional hypotheses generated by the direct and indirect pathways framework, no study has attempted to reconcile the very well classified striatal type IIb neurons (Liles, 1979; Crutcher and DeLong, 1984a; Alexander and DeLong, 1985; Liles, 1985; Liles and Updyke, 1985; Kimura, 1990; West et al., 1990; Carelli and West, 1991; Cho and West, 1997) with the primary functional tenet of the direct and indirect pathway hypothesis: that Drd1 neurons should be active during movement, while Drd2 neuron activity should be related somehow to non-movement of body parts. Based on the canonical theory alone, one might predict that striatal type IIb neurons are all Drd1 expressing MSNs which project in the direct pathway. However, the above evidence of Drd2 MSN activation during movement (Cui et al., 2013) suggests that it is possible that both Drd1

and Drd2 MSNs could be type IIb neurons, i.e. neurons that increase firing during movement of a related body part. Such a result would provide further evidence that the direct and indirect pathways hypothesis needs to be updated.

In the present study, we sought to fill the aforementioned gap in the literature by recording the activity of single neurons in the DLS of freely moving Drd1-Cre and Drd2-Cre mice and by employing a somatosensorimotor exam after an optogenetic identification procedure. At the onset of this study a great deal of information was already known about the neurons being recorded. It was known that 1) a recorded neuron exhibiting a slow spike waveform and low baseline firing rate is nearly 100% likely to be an MSN; 2) of neurons meeting these criteria, those that exhibit activity related to sensorimotor activity of body parts are type IIb projection neurons (Kimura et al., 1990) that receive glutamatergic input from S1/M1 (Liles and Updyke, 1985) and dopaminergic input from SNc (Freund et al., 1984). Using the aforementioned techniques, we were also able to produce a great deal more information about these neurons. We were able to 1) determine unambiguously through optogenetic identification if a neuron expressed Drd1 or Drd2 and 2) determine whether a neuron outputs through the direct or indirect pathway though histological verification of axon tracts, and 3) we could determine for the first time if type IIb neurons reside in the direct and/or indirect pathways. Interpretations from this study are thus firmly grounded in the knowledge of neuron type, the neuron's specific S1/M1 afferents, its palidal efferents, as well as its DA receptor expression.

Methods

Subjects

Adult mice (N = 15) were used in this study. Five wild type C57/BL6 mice were used as optogenetics controls, and helped us determine the validity of body exams in the mouse. Two strains of transgenic Cre-driver mice were used in order to facilitate optogenetic identification of Drd1 and Drd2 expressing neurons. Breeding pairs of Drd1-Cre [B6.Cg-Tg(Drd1-Cre)262Gsat/Mmcd] and Drd2-Cre [B6.FVB(Cg)-Tg(Drd2-Cre)ER44Gsat/Mmcd] were purchased from the UC Davis Mutant Mouse Research and Resource Center (MMRRC, Davis, CA), and back bred to C57/BL6 in order to produce heterozygous Drd1-Cre and Drd2-Cre animals for experimentation. Five Drd1 and 5 Drd2 animals were utilized in this study.

Viral Vector

An adeno-associated virus (AAV-EF1a-FLEx-Chronos-GFP; UNC Vector Core, Chapel Hill, NC) was used to express a light sensitive cation channel (Chronos-GFP) in the presence of Cre (Klapoetke et al., 2014). This is achieved by FLEX recombination of the transgene, which changes the orientation of the coding sequence with respect to the promoter such that the protein may be expressed. In the present animals, the Cre enzyme was selectively expressed in either Drd1 or Drd2 expressing neurons. Accordingly, Chronos-GFP expression was limited to those neurons. Chronos-GFP could only express in Drd1 neurons in a Drd1-Cre animal and in Drd2 neurons in a Drd2-Cre animal. To limit spatial spread of Chronos-GFP, the AAV was intra-cranially microinjected into the dorsolateral striatum (described below; Fig. 1d).

Surgery

Mice (25-30g) were anesthetized and surgically prepared for chronic, extracellular single unit recording as described previously (Barker et al., 2014) using a fully automated stereotaxic instrument (Coffey et al., 2013). Each animal was intra-cranially injected with 1ul of AAV-EF1a-FLEX-Chronos-GFP at the following coordinates relative to bregma over 10 minutes (ML 2.5mm, AP 0.5mm, DV -2.75mm). Following injections, animals were implanted with an array of 15x 25µm stainless steel micro-wires (Micro-Probes, Gaithersburg, MD) surrounding a 200µm, 39NA, optical fiber (Thor Labs; Newton, NJ) through the same craniotomy. The micro-wires extended 300µm ventral to the tip of the optical fiber and a maximum of 500µm laterally from the center of the optical fiber, allowing for illumination of the entire wire array (Fig. 1a). Opto-arrays were lowered using a motorized stereotaxic device (Coffey et al., 2013) at a rate of 200µm/min and to a depth of 2.75mm below the surface of the skull. The array was sealed to the surface of the skull with cyanoacrylate. The wires lead to a connector strip embedded in dental cement on the skull. Animals were given one week to recover from surgery, and had ad lib access to food and water at all times (Fig. 1c).

Electrophysiological Recording

When recording commenced, a recording harness (Triangle Biosystems; Durham, NC) connected to a commutator was attached to the connector strip on the skull, allowing free movement within the Plexiglas recording chamber (25cm x 40cm x 40cm). Signals were amplified and filtered (450 Hz to 10 kHz; roll off 1.5 dB/octave at 1 kHz and -6 dB/octave at 11 kHz), and digitized (50 kHz sampling frequency per wire) for off-line

analysis (DataWave Technologies; Loveland, CO). Protocols were performed in compliance with the *Guide for the care and use of laboratory animals* (NIH Publication 865-23) and were approved by the Institutional Animal Care and Use Committee, Rutgers University.

Optogenetic Identification of Drd1 & Drd2 Receptor Expressing Neurons

Light stimulation consisted of a 1m baseline recording period, followed by 4 blocks of light stimulation at increasing intensities, ranging from 0.1mW to 03.0mW (1–25 mW/mm^2; Kravits et al., 2013). Each stimulation block consisted of 100x 5ms light pulses delivered at 1Hz. Each block was separated by a 1m "laser-off" interval. To determine if neurons were light sensitive, a baseline firing rate (FR) and standard deviation were calculated for each single neuron from the 1m baseline recording as well as all "laser-off" intervals. If a neuron's average FR during the 5ms light stimulations, in any intensity block, exceeded its 99.5% confidence interval from baseline, it was deemed light sensitive (Kravits et al., 2013). Any neurons deemed light sensitive in Drd1-Cre animals were identified as Drd1 expressing neurons of the direct pathway, and any neurons deemed light sensitive in Drd2-Cre animals were identified as Drd2 expressing neurons of the indirect pathway.

Body Exam

Procedures for conducting the somatosensorimotor exam were similar to those used recently in a study of mice (Coffey et al., 2016) and previously in rats (Carelli and West, 1991; Cho and West, 1997; Prokopenko et al., 2004). The change in FR of a type IIb neuron during activity of the related body part is uniformly an increase. Therefore,

animals were trained to remain still, resulting in low baseline FRs of DLS MSNs. Body exams required weeks of patient, daily handling. The exam was conducted in its entirety and video recorded over several sessions (approximately 2hr/session). Multiple stimuli (at least 10) of each type were applied to each body part. Cutaneous stimulation was delivered via a handheld probe (2mm in diameter), calibrated to deliver 2-4g of force. The probe travels a distance of up to 3cm in 0.15-0.5s. All accessible body parts (head, vibrissae, paw, chest, chin, snout, ear, shoulder, cheek pad, and trunk) underwent stimulation of various types, e.g., cutaneous touch, passive manipulation, and active movement. Body parts were observed during active movement, were tapped with the probe, and the fur or skin was gently palpated. Passive manipulation was applied to the limbs and neck. The latter, achieved by gently manipulating the harness, was used to identify neurons related to head movement. Firing in relation to the snout, chin or trunk was evaluated using cutaneous stimulation. Testing of the shoulder consisted of cutaneous stimulation, palpation, either manually or with the probe, and passive rotation. Vibrissae collectively were stimulated by stroking with the probe forward, backward, up and down. Multiple stimuli (at least 10) of each type were applied to each body part, and stimuli were presented 3 to 10s apart. All types of manipulation are referred to here as “stimulation”. Habituation was minimized by the continual shifting of stimulation to different body parts in different sequences.

Video Analysis

Video recordings time stamped by the computer which also recorded neural activity (Datawave Video Bench; Loveland, CO) were obtained during every exam. They

enable unambiguous identification (33ms resolution) of the onset and offset of each individual stimulus using post-hoc frame-by-frame (30 frames/s) analysis. The onset of each movement or touch was defined as the timestamp of the video frame immediately prior to the frame that first captured body part movement or touch, while offset was defined as the timestamp of the first video frame after the frame that captured the end of body part movement or touch. Video analysis was used to filter out trials containing extraneous events, such as movements of non-stimulated body parts. This "purification" of stimuli, to the extent possible, enabled a clear depiction of a difference between Stimulation FR vs Baseline FR with as few as 10 nodes. When more than one body part moved on a given trial, not only did we discard the trial and select trials lacking extraneous movements, we also examined trials that isolated stimulation of the extraneous body part, in order to verify lack of responsiveness. The protocols described here are the same as those that were effective in our recent identification of DLS neurons related to body parts in wild type mice (Coffey et al., 2016).

Identifying Type IIb Medium Spiny Neurons with Firing Related to Body Part Stimulation

Rasters and peri-event time histograms (PETHs) displaying FR of individual neurons were constructed using video-defined nodes. For each neuron, raster-PETHs corresponding to all examined body parts were created. The mean Stimulus FR was defined as the average FR during body part stimulation, i.e., between all onset-to-offset nodes set during video analysis. The mean and standard deviation for Baseline FR were calculated during all periods of non-stimulation by the experimenter, during which time the animals were not moving. Average FR during the stimulus was compared to Baseline

FR and baseline variance. Each neuron was tested for sensitivity to 10 body parts, so the alpha value for determining sensitivity was Bonferroni corrected from 0.05 to 0.005. Any Stimulus FR exceeding the neuron's 99.5% confidence interval for Baseline FR was deemed to be a type IIb medium spiny neuron.

Fluorescent Immunohistochemical Labeling

Following all recordings (~30 days after surgery) animals received an overdose of sodium pentobarbital and were perfused transcardially with 0.9% phosphate buffered saline followed by 4% paraformaldehyde. Brains were post-fixed for 48 hours in 4% paraformaldehyde and transferred to a 30% sucrose solution. Brains were sliced into 30 µm coronal sections. Fluorescent immunohistochemistry was performed on free floating brain tissue. Slices were incubated for one hour in a 4% Bovine Serum Albumin (BSA) and 0.3% Triton X-100 in phosphate buffer. Sections were rinsed and incubated overnight in a 4% BSA with rabbit anti-GFAP antibody. Next, tissue was rinsed and incubated in anti-rabbit secondary antibody conjugated to a red fluorophore (Alexa Fluor ® 555). Subsequently, tissue was washed with phosphate buffer and mounted on a slide using mounting medium containing Dapi (nucleic acid stain), which serves as a counter stain. All slices were photographed and recorded with a Zeiss Axiovert 200M, Fluorescence microscope. The presence of astrocytes with upregulated GFAP along the entire length of microwires and the fiber optic allowed tracing of microwire tracks by staining for GFAP protein (Polikov, 2006; Fig. 1 inset). If all 15 wires could not be tracked from their entrance into the cortex to their tips in the DLS, data from that animal were discarded.

Direct and Indirect Pathway Reconstruction

One Drd1 animal and one Drd2 animal were used to reconstruct the striato-pallidal projections of the direct and indirect pathways. Each animal was injected with 1µl of AAV-EF1a-FLEX-Chronos-GFP in the right DLS (see "*Surgery"* for coordinates). Animals were housed for 2 months to allow for the AAV to infect striatal projection neurons, and to produce GFP all the way down to their terminals. Following 2 months the animals were sacrificed and their brains were sliced coronally at 100µm thickness for the extent of the striatum and globus pallidus. The slices were then serially mounted and imaged in high resolution. To ensure the highest resolution possible for tracking projections, each coronal section was imaged in 9 overlapping frames under a 4x objective and then stitched back together using an automated stitching algorithm (Image J; Preibisch et al., 2009). Each coronal section was then aligned using an automated image alignment algorithm (Image j; Thévenaz et al., 1998). Aligned images could then be scrolled through or reconstructed in 3D.

Results

Viral Tract Tracing and Histological Verification of Wire Tips

AAV-EF1a-FLEX-Chronos-GFP injected into the dorsolateral striatum of a Drd1-Cre mouse resulted in expression of Chronos-GFP in Drd1 MSNs within dorsolateral striatum. Because Chronos-GFP is expressed highly in the soma, axon and terminal, it is possible to track the projections of Drd1 MSNs into the globus pallidus internal segment (GPi) and the substantia nigra reticulata (SNr; Fig. 2a). These projections were totally consistent with the theorized output of the direct pathway. AAV-EF1a-FLEX-Chronos-GFP injected into the dorsolateral striatum of a Drd2-Cre mouse resulted in expression of Chronos-GFP in Drd2 MSNs within dorsolateral striatum and projection into the globus pallidus external segment (GPe). This was also totally consistent with the theorized output of the indirect pathway (Fig. 2b). AAV-EF1a-FLEX-Chronos-GFP injected into the dorsolateral striatum of wild type (WT) mice never produced detectable levels of Chronos-GFP expression in the dorsolateral striatum (data not shown).

For all Drd1-Cre and Drd2-Cre experimental mice, viral expression was verified through coronal sectioning and fluorescent imaging of the dorsolateral striatum. Viral expression was also used to verify the output pathway of Chronos-GFP expressing neurons for all experimental animals. Chronos-GFP expressed in Drd1-Cre mice projected exclusively to the GPi (Fig. 3a,c), whereas in Drd2-Cre mice Chronos-GFP projected exclusively to the GPe (Fig. 3b,d). These extremely consistent results support the hypothesis that Drd1 neurons and Drd2 neurons have segregated output pathways. They also further justify the use of Drd1-Cre and Drd2-Cre mice to model and study the

functional differences between neurons residing in the direct and indirect output pathways of the dorsolateral striatum.

Summary of All Wires Implanted into the Dorsolateral Striatum

Histology confirmed the location of all 15 wires in the 5 wild type animals. All 15 wires were tracked to the DLS in 4 Drd1-Cre animals (1 animal was removed), and all 15 wires were tracked to the DLS in 3 Drd2-Cre animals (2 animals were removed). In total, 12 mice including of 5 WT, 4 Drd1-Cre, and 3 Drd2-Cre, implanted with 180 microwires, were used in the study. Of the 180 wires implanted, 125 yielded neural recordings. Of those 125 recorded neurons, 99 were not identified to be Drd1 or Drd2 expressing. Thirteen neurons were identified as Drd1 expressing MSNs and another 13 neurons were identified as Drd2 expressing MSNs. Fifty-five wires yielded no recorded neurons (Fig. 4a).

Type IIb Medium Spiny Neurons in the Mouse Dorsolateral Striatum

Type IIb medium spiny neurons in the mouse dorsolateral striatum exhibited selective responses to body part stimulation. The responses of these neurons to body part stimulation were not totally uniform, but they all share some remarkably consistent features. First, type IIb neurons have a low and stable baseline firing rate (~1 spike/s) while animals were not moving, likely because of minimal cortical glutamatergic input at rest. Second, responses from type IIb neurons' always consisted of an increase in firing rate (~7 spikes/s) relative to their baseline upon stimulation of the correlated body part. Third, for all body parts, type IIb neurons increased firing rate only *during* stimulation

(e.g., not before movement onset) and decreased back to baseline quickly at the offset of stimulation. This pattern was consistent across all body parts (Fig. 5).

Of the 99 neurons where dopamine receptor type was unknown (unidentified neurons), 61 neurons were not categorized as being type IIb neurons with firing related to body part stimulation. Thirty-eight neurons were deemed sensitive to single body part stimulation and categorized as type IIb neurons. One neuron each fired in relation to trunk, contralateral shoulder, contralateral paw, and contralateral ear stimulation; 2 neurons fired in relation to contralateral cheek stimulation; 3 neurons fired in relation to contralateral vibrissae stimulation; 4 neurons fired in relation to head movement in a downward direction; 5 neurons fired in relation to head movement toward the left; 5 neurons fired in relation to chest stimulation; 5 neurons fired in relation to stimulation of the snout; 6 neurons fired in relation to chin stimulation and 6 neurons fired in relation to head movement toward the right (Fig. 4b).

Drd1 and Drd2 Optogenetic Identification

Optogenetic identification procedures never produced a neuron sensitive to light stimulation in WT animals. This result was corroborated by a total lack of viral expression in the wild type animals. Without the Cre enzyme, AAV-EF1a-FLEX-Chronos-GFP cannot infect cells. As such, neurons remain insensitive to very short bursts of light stimulation. In Drd1-Cre animals, 13 neurons were deemed sensitive to light stimulation (Fig. 6a), and in Drd2-Cre animals, 13 neurons were deemed sensitive to light stimulation (Fig. 6b). Neurons that were sensitive to light stimulation increased firing beyond their 99.5% confidence interval during the 5ms “laser on” periods. While the

pattern of activation during light stimulation was highly varied (Fig. 6) neurons that responded consistently during the 5ms light pulse must have incorporated Chronos-GFP into their cell membrane. Using a short light pulse ensured that it was impossible for surrounding GABAergic MSNs to increase (e.g., disinhibit) the firing rate of the recorded MSN within 5ms. Thus, the light sensitive MSNs are guaranteed to express Drd1 in Drd1-Cre animals and Drd2 in Drd2-Cre animals. Further, from histological verification of axon terminals, we can be confident that light sensitive neurons in Drd1-Cre animals project through the direct pathway to the GPi while light sensitive neurons in Drd2-Cre animals project through the indirect pathway to the GPe.

Both Drd1 and Drd2 MSNs can be Type IIb Medium Spiny Neurons

The 26 type IIb MSNs in Drd1-Cre and Drd2-Cre animals were identified with the same criteria as the WT neurons. Of the 13 identified Drd1 neurons, 7 were not categorized as type IIb neurons, and did not exhibit firing related to body part stimulation. Of the 6 remaining Drd1 neurons, 1 neuron fired in relation to head movement in the upward direction, 1 neuron fired in relation to head movement to the left, 1 neuron fired in relation to snout stimulation, 1 neuron fired in relation to contralateral cheek stimulation (Fig. 7b), and lastly, 2 neurons fired in relation to trunk stimulation (Fig. 7a). Of the 13 identified Drd2 neurons, 6 were not categorized as type IIb neurons. Of the remaining 7 Drd2 expressing neurons, 1 neuron fired in relation to chin stimulation, 1 fired in relation to contralateral shoulder stimulation, 1 fired in relation to contralateral vibrissae stimulation (Fig. 8a), 1 fired in relation to head

movement in a downward direction, 1 fired in relation to head movement in the upward direction, and 2 neurons fired in relation to snout stimulation (Fig. 8b).

Summary of Type IIb Medium Spiny Neurons

All type IIb neurons processed body part stimulation similarly whether they were unidentified, Drd1 expressing, or Drd2 expressing (Fig. 9). Unidentified type IIb neurons on average, increased firing rate from 0.75 spikes/s during baseline to 7.95 spikes/s during body part stimulation. Drd1 type IIb neurons on average increased firing rate from 1.65 spikes/s during baseline to 7.91 spikes/s during stimulation. Drd2 type IIb neurons, on average, increased firing rate from 1.24 spikes/s during baseline to 7.89 spike/s during stimulation. We observed no significant difference in stimulation firing rate between all 3 categories of type IIb neurons. Unidentified type IIb neurons' firing rate during stimulation did not differ from that of Drd1 type IIb neurons [KS=0.33, p=0.57]. Unidentified type IIb neurons' firing rate during stimulation did not differ from that of Drd2 type IIb neurons [KS=0.27, p=0.75]. Drd1 type IIb neurons' firing rate during stimulation did not differ from that of Drd2 SBP neurons [KS=0.26, p=0.85]. Non-type IIb MSNs exhibited no difference in firing rate between baseline and stimulation [KS=.35, p=.68].

Selectivity of Type IIb Medium Spiny Neurons

Type IIb neurons fire during stimulation of a particular body part, but not during stimulation of other body parts (Fig. 10). Furthermore, neurons that process head movement were even selective for a single direction. No neurons that processed upward head movement also processed another direction. The extent of this selectivity

can be easily visualized (Fig. 11). Each row in the heat map represents a single neuron and each column represents a body part. Firing rate during stimulation for each neuron is converted to sigma (standard deviations from baseline firing rate) and coded in color. Each neuron's correlated body part is aligned to the right column, while each unrelated body part is shown in the remaining columns, sorted from most to least (right-to-left) firing during stimulation. All type IIb neurons fired highly selectively during stimulation of their correlated body part and fired minimally during all other body part stimulations. Some neurons even broke 20 standard deviations (sigma) from baseline during related body part stimulation, while the closest non-related body parts never broke 3 standard deviations. No type IIb neuron in this study was identified as being related to more than one body part.

Discussion

Type IIb Neurons in the Mouse Dorsolateral Striatum

To the best of our knowledge, this study was the first to systematically study type IIb neurons in the direct and indirect pathways of the mouse striatum. In doing so, we have confirmed that the dorsolateral striatum in the mouse brain has an analogous sensorimotor function to that shown in primates (Liles, 1979; Crutcher and DeLong, 1984a; Alexander and DeLong, 1985; Lyles and Updyke, 1985) and rats (West et al., 1990; Carelli and West, 1991; Cho and West, 1997). These neurons also show remarkable consistency with previous studies, especially those in the rat. For example, 55 of 125 (40.8%) neurons in this study were found to fire in relation to single body part stimulation. This is nearly identical to the ratio of type IIb neurons (524 of 1287; 41%) found in a larger sample of rat DLS neurons (Cho and West, 1997). Furthermore, although the sample of Drd1 and Drd2 neurons was relatively small, both groups showed similar ratios of type IIb neurons (45~55%). Finally, type IIb MSNs in the mouse striatum are selective for a single body part and direction of movement, as they are in the rat (Cho and West, 1997; Carelli and West, 1991). Indeed, compared to the DLS of the rat and primate, no quantitative or qualitative differences were observed for type IIb neurons of the mouse dorsolateral striatum, the importance of which is discussed below.

Importance of the Mouse Model

The consistency of this study with previous studies in multiple species further validates the use of the mouse model for studying the sensorimotor functions of the

dorsolateral striatum. This is essential for the neuroscience field, as the mouse has unparalleled access to modern genetic neuroscience toolkits. These tools include but are not limited to transgenic mice, Cre-driver lines, optogenetics, and DREADDs. Toolkits like these give researchers precise control over the types of neurons they are visualizing, manipulating, recording, etc. Because of these toolkits, recent studies have already opted to utilize the mouse to study the function of the striatum and the direct and indirect pathways (e.g., Kravitz et al., 2010; Cazorla et al., 2014; Cui et al., 2013). However, it is important that future studies of the dorsolateral striatum during behavioral tasks address the contribution of type IIb neurons. Combining all striatal neurons together for analysis (i.e., neurons having no apparent sensorimotor processing) with neurons that process different body parts, while at the same time ignoring their different body part sensitivities, creates a risk of throwing out a layer of complexity that the striatum is known to possess, and could yield uninterpretable results.

Drd1-Cre and Drd2-Cre Mice Are Valid Models of the Direct and Indirect Pathways

Drd1-Cre and Drd2-Cre mice have repeatedly been shown to satisfy the anatomical tenets of the direct and indirect pathways: that Drd1 and Drd2 are segregated on separate medium spiny neurons and that Drd1 and Drd2 MSN outputs are segregated between the direct (GPi-SNr) and indirect (GPe) pathways. While some older studies utilizing immunohistochemistry have shown significant overlap in Drd1 and Drd2 (Aizman et al., 2000), more modern studies that rely on the Drd1 and Drd2 promoters have shown minimal overlap between neurons (~2-5%; Bertran-Gonzalez et

al., 2008; Thibault et al., 2013). These studies also show that Drd1 and Drd2 neurons exist in roughly equal proportions in the DLS (52% Drd1 & 43% Drd2). In the present study, we have confirmed that Drd1 MSNs in the DLS project en masse to the GPi and SNr, while Drd2 MSNs projects en masse to GPe. While it is possible that some neurons may collateralize in both output nuclei (Parent et al., 1995), it is clear from our own histology, as well as the histology of other studies, that Drd1 and Drd2 MSNs in the dorsolateral striatum have segregated output pathways which show remarkable consistency with the hypothesizes direct and indirect pathways (Gerfen et al., 2008, Cui et al., 2013; Wall et al., 2013; Kravitz et al., 2010; Cazorla et al., 2014).

Drd1 and Drd2 MSNs Can Be Identified Unambiguously

Performing in-vivo electrophysiological studies once precluded researchers from determining the chemical anatomy of the neurons from which they were recording. However, with the combined advances of the Cre-LoxP recombinase system and Optogenetics, recorded neurons can now be identified with a high degree of confidence. The reasons for this degree confidence are as follows. First, the Cre-LoxP system is a highly efficient method of delivering genetic material to the exact cell type of interest. The present study used Drd1-Cre and Drd2-Cre mice, which are well categorized and highly representative of endogenous Drd1 and Drd2 in the direct and indirect pathways (Gerfen et al., 2008). These mice allowed us to insert an opsin and fluorophore into either Drd1 or Drd2 neurons. Second, we were able to unambiguously identify those neurons by their response to a brief 5ms light pulse. We chose a very conservative identification procedure with a short light pulse to ensure that the neurons classified as

Drd1 and Drd2 MSNs were in fact directly sensitive to the light stimulation, and not to secondary stimulation (e.g. through multisynaptic activation). Any neuron that was active during light stimulation (>99.5% CI; Kravitz et al., 2013) must have incorporated light sensitive opsins, and therefore must express Drd1 or Drd2. Finally, every animal's brain was dissected to determine if the opsin expressing neurons in Drd1 animals projected to GPi, and if the opsin expressing neurons in Drd2 animals projected to GPe. This final step crystalized our confidence in the identification of neurons as direct (Drd1) or indirect (Drd2) pathway MSNs.

Type IIb MSNs Reside in Both the Direct (Drd1) and Indirect (Drd2) Pathways

Given the substantial anatomical differences between Drd1 and Drd2 MSNs, as well as their hypothesized functional differences, it was predicted that Drd1 and Drd2 neurons would process body part stimulation differently. However, both Drd1 and Drd2 MSNs type IIb neurons processed single body part stimulation similarly. First, roughly the same proportion (~50%) of Drd1 and Drd2 MSNs were classified as body part sensitive type IIb MSNs, which matches the ratio of body part sensitive neurons in the wild type mouse, as well as in rats and monkeys. Second, both Drd1 and Drd2 type IIb neurons had similar baseline firing rates (~1hz) and stimulation firing rates (~8hz), and both were similar to the wild type mouse. Finally, both Drd1 and Drd2 neurons showed complete selectivity to a single body part. No neuron in either group was classified as a type IIb neuron related to more than one body part. These results are consistent with the observation that both Drd1 and Drd2 MSNs in dorsolateral striatum receive the bulk of their excitatory input from primary motor and somatosensory cortex.

Functional Tenets of the Direct and Indirect Pathways Hypothesis

Our result, that both Drd1 and Drd2 neurons increase firing rate during stimulation, is consistent with what is known about striatal MSN input. However, it is harder to reconcile this result with the leading functional tenet of the direct and indirect pathways hypothesis: that activation of the direct pathway produces movement, while activation of the indirect pathway inhibits movement. There is one piece of experimental evidence (Kravitz et al., 2010) which shows that activation of large ensembles of Drd1 neurons produces locomotion, while activation of large ensembles of Drd2 neurons produces freezing. However, it is difficult to understand how indiscriminate activation of many Drd1 MSNs, which ostensibly process different body parts, would result in a coordinated activity such as locomotion, while indiscriminate activation of Drd2 MSNs could produce freezing either through inhibition of muscles, or through activation of too many opposing muscles.

Since then, other studies have shown that both Drd1 and Drd2 neurons are active together during movement (Cui et al., 2013), and that their cooperation is necessary for refining motion. There has been an attempt to fit this result into the current model by proposing that to perform certain actions (e.g. locomotion), all other actions (e.g. grooming) must be inhibited. However, our results suggest that DLS neurons process information at the level of individual body parts, and not at the level of coordinated action among body parts, a property characteristic of firing throughout the S1/M1 corticostriatal-pallidothalamocortical reentrant loop. A further discrepancy is revealed by the main finding of the present study: similar increases in firing, or

collaboration, between Drd1 and Drd2 neurons during sensorimotor stimulation. For a Drd2 neuron to inhibit movements other than its related movement, its target neurons in pallidum would have to be responsive to body parts other than the one currently moving. Importantly, no such result has ever been reported. In fact, the specificity of phasic firing in relation to movement around an individual joint is similar between GPi and GPe neurons (Iansek and Porter, 1980; Erez et al, 2011), and is lost only in disease models (Filion et al 1988; Rothblat and Schneider, 1995). Thus, it seems likely that the functional aspect of the direct and indirect pathways hypothesis is either overly simplistic or incorrect. That begs the question, why do the direct and indirect pathways have segregated receptor type and output nuclei if they fire similarly and process the same information?

An Alternate Explanation for Parallel Processing in Drd1 and Drd2 Neurons

While there are numerous possible explanations for the segregation of Drd1 and Drd2 MSN outputs, one stands out considering the role of dorsolateral striatum as a sensorimotor integrator for refining ongoing movement. It is known that type IIb MSNs in the dorsolateral striatum exhibit firing rates correlated to some parameters of movement. Using velocity as an example, type IIb neurons in the direct pathway may send current velocity information “directly” to the thalamus. The indirect pathway, on the other hand, projects through more synapses and becomes inhibitory before reaching the motor thalamus a few milliseconds later. Type IIb MSNs in the indirect pathway could send a time lagged and inverted (inhibitory) copy of the velocity signal to thalamus, such that the thalamus can compute the difference between the current

velocity and the immediately preceding velocity of the movement. This effectively allows the thalamus to compute movement onset, offset, and acceleration from two time lagged velocity signals (Fig. 12). This kind of process could be useful in refining an ongoing movement, as the striatum could easily compare current and previous movement parameters (position, direction, velocity, etc.) and make corrections to trajectory. While this is speculation, it is consistent with the present findings and seems more parsimonious with the existing evidence than the canonical "go-/-no-go" hypothesis, or the more modern "promote movement / inhibit competing movements" hypothesis.

Conclusion

This study provides further evidence that Drd1-Cre and Drd2-Cre animals are valid models of the direct and indirect pathways of the striatum. Using these animals, combined with optogenetics and electrophysiology, we were able to unambiguously identify Drd1 and Drd2 MSNs in the striatum of awake, behaving, mice. We then studied those neurons with regard to single body part processing. While type IIb neurons have been well characterized in other species, they were only recently characterized in the mouse (Coffey et al., 2016). It may have been presumed that these neurons would reside only in the direct pathway, which was thought to promote movement. However, we are the first to show that both the direct and indirect pathways contain type IIb neurons, whose firing rates are related to stimulation of individual body parts. This evidence, combined with a number of other recent studies, brings into question the decades old functional aspect of the direct and indirect pathways hypothesis: that Drd1

neurons promote movement, while Drd2 neurons inhibit it. Rather, Drd1 and Drd2 neurons appear to process sensorimotor information similarly, and both Drd1 and Drd2 neurons fire during body part stimulation and movement. These results suggest that while the anatomical aspects of the direct and indirect pathways hypothesis are highly corroborated, the functional aspect needs a critical reevaluation.

References

Aizman, O., Brismar, H., Uhlén, P., Zettergren, E., Levey, A. I., Forssberg, H., & Aperia, A. 2000. Anatomical and physiological evidence for D1 and D2 dopamine receptor colocalization in neostriatal neurons. Nature Neurosci. 3(3), 226-230.

Albin, R.L., Young, A.B., & Penney, J.B. 1989. The functional anatomy of basal ganglia disorders. Trends in Neurosci. 12(10), 366-375.

Alexander, G.E., & Delong, M.R. 1985. Microstimulation of the primate neostriatum. II. Somatotopic organization of striatal microexcitable zones and their relation to neuronal response properties. J. Neurophys. 53, 1417-1430.

Alexander, G.E., DeLong, M.R., & Strick, P.L. 1986. Parallel organization of functionally segregated circuits linking basal ganglia and cortex. Ann. Rev. of Neurosci. 9(1), 357-381.

Alexander, G.E., & Crutcher, M.D. 1990. Functional architecture of basal ganglia circuits: neural substrates of parallel processing. Trends in Neurosci. 13(7), 266-271.

Barker, D.J., Coffey, K.R., Ma S., Root, D.H., & West, M.O. 2014. A Procedure for Implanting Organized Arrays of Microwires for Single-Unit Recordings in the Awake, Behaving Animal. J. Vis. Exp. 84, e51004.

Bertran-Gonzalez, J., Bosch, C., Maroteaux, M., Matamales, M., Hervé, D., Valjent, E., & Girault, J.A. 2008. Opposing patterns of signaling activation in dopamine D1 and D2 receptor-expressing striatal neurons in response to cocaine and haloperidol. J. Neurosci. 28(22), 5671-5685.

Carelli, R.M., & West, M.O. 1991. Representation of the body by single neurons in the dorsolateral striatum of the awake, unrestrained rat. J. Comp. Neurol. 309, 231-249.

Cazorla, M., de Carvalho, F.D., Chohan, M.O., Shegda, M., Chuhma, N., Rayport, S., & Kellendonk, C. 2014. Dopamine D2 receptors regulate the anatomical and functional balance of basal ganglia circuitry. Neuron. 81(1), 153-164.

Cho, J., & West, M.O. 1997. Distributions of single neurons related to body parts in the lateral striatum of the rat. Brain Res. 756, 241-246.

Coffey, K.R., Barker, D.J., Ma, S., & West, M.O. 2013. Building an open-source robotic stereotaxic instrument. J. Vis. Exp. 80, e51006.

Coffey, K.R., Nader, M., & West, M.O. 2016. Single body parts are processed by individual neurons in the mouse dorsolateral striatum. Brain Res. 1636, 200-207.

Cospito, J.A., & Kultas-Ilinsky, K. 1981. Synaptic organization of motor corticostriatal projections in the rat. Exp. Neurol. 72, 257-266.

Crutcher, M.D., & Delong, M.R. 1984. Single cell studies of the primate putamen. I. Functional organization. Exp. Brain. Res. 53, 233-243.

Cui, G., Jun, S. B., Jin, X., Pham, M.D., Vogel, S.S., Lovinger, D.M., & Costa, R.M. 2013. Concurrent activation of striatal direct and indirect pathways during action initiation. Nature. 494(7436), 238-242.

Erez Y., Tischler H., Belelovsky K., & Bar-Gad I. 2011. Dispersed activity during passive movement in the globus pallidus of the 1-methyl-4-phenyl-1,2,3,6-tetrahydropyridine (MPTP)-treated primate. PLoS One. 6(1), e16293.

Filion M., Tremblay L., & Bedard P.J. 1988. Abnormal influences of passive limb movement on the activity of globus pallidus neurons in parkinsonian monkeys. Brain Res. 444, 165-176.

Flaherty, A.W., & Graybiel, A.M. 1993. Two input systems for body representations in the primate striatal matrix: experimental evidence in the squirrel monkey. J. Neurosci. 13, 1120-1137.

Flaherty, A.W., Graybiel, A.M. 1994. Input-output organization of the sensorimotor striatum in the squirrel monkey. J. Neurosci. 14, 599-610.

Frederick, A.L., Yano, H., Trifilieff, P., Vishwasrao, H.D., Biezonski, D., Mészáros, J., & Graham, D.L. 2015. Evidence against dopamine D1/D2 receptor heteromers. Mol. Psychi. 1, 1-10

Freund, T.F., Powell, J.F., & Smith, A.D. 1984. Tyrosine hydroxylase-immunoreactive boutons in synaptic contact with identified striatonigral neurons, with particular reference to dendritic spines. Neurosci. 13(4), 1189-1215.

Friend, D.M., & Kravitz, A.V. 2014. Working together: basal ganglia pathways in action selection. Trends in Neurosci. 37(6), 301-303.

Gerfen, C.R., Engber, T.M., Mahan, L.C., Susel, Z., Chase, T.N., Monsma, F.J., & Sibley, D.R. 1990. D1 and D2 dopamine receptor-regulated gene expression of striatonigral and striatopallidal neurons. Science. 250(4986), 1429-1432.

Gerfen, C.R., Paletzki, R., & Heintz, N. 2013. GENSAT BAC Cre-recombinase driver lines to study the functional organization of cerebral cortical and basal ganglia circuits. Neuron. 80(6), 1368-1383.

Gong, S., Doughty, M., Harbaugh, C.R., Cummins, A., Hatten, M.E., Heintz, N., & Gerfen, C.R. 2007. Targeting Cre recombinase to specific neuron populations with bacterial artificial chromosome constructs. J. Neurosci. 27(37), 9817-9823.

Hattox, A.M., & Nelson, S.B. 2007. Layer V neurons in mouse cortex projecting to different targets have distinct physiological properties. J. Neurophysiol. 98(6), 3330-40.

Iansek R., Porter R., 1980. The monkey globus pallidus: neuronal discharge properties in relation to movement. J. Physiol. 301, 439-455.

Jinno, S., & Kosaka, T. 2004. Parvalbumin is expressed in glutamatergic and GABAergic corticostriatal pathway in mice. J. Comp. Neurol. 477(2), 188-201.

Kimura, M., Kato, M., & Shimazaki, H. 1990. Physiological properties of projection neurons in the monkey striatum to the globus pallidus. Exp. Brain. Res. 82, 672-676.

Klapoetke, N.C., Murata, Y., Kim, S.S., Pulver, S.R., Birdsey-Benson, A., Cho, Y.K., & Wang, J. 2014. Independent optical excitation of distinct neural populations. Nature Meth. 11(3), 338-346.

Kravitz, A.V., Freeze, B.S., Parker, P.R., Kay, K., Thwin, M.T., Deisseroth, K., & Kreitzer, A.C. 2010. Regulation of parkinsonian motor behaviours by optogenetic control of basal ganglia circuitry. Nature. 466(7306), 622-626.

Kravitz, A.V., Owen, S.F., & Kreitzer, A.C. 2013. Optogenetic identification of striatal projection neuron subtypes during in vivo recordings. Brain Res. 1511, 21-32.

Kunzle, H. 1975. Bilateral projections from precentral motor cortex to the putamen and

other parts of the basal ganglia: An autoradiographic study in Macaca fascicularis. Brain. Res. 88, 195-209.

Kunzle, H. 1977. Projections from the primary somatosensory cortex to basal ganglia and thalamus in the monkey. Exp. Brain. Res. 30, 481-492.

Lemos, J.C., Friend, D.M., Kaplan, A.R., Shin, J.H., Rubinstein, M., Kravitz, A.V., & Alvarez, V.A. 2016. Enhanced GABA Transmission Drives Bradykinesia Following Loss of Dopamine D2 Receptor Signaling. Neuron. 90(4), 824-838.

Lévesque, M., & Parent, A. 2005. The striatofugal fiber system in primates: a reevaluation of its organization based on single-axon tracing studies. PNAS. 102(33), 11888-11893.

Liles, S.L. 1979. Topographic organization of neurons related to arm movement in the putamen. In: Advances in Neurology. Chase TN, (ed). Raven Press, New York.

Liles, S.L., & Updyke, B.V. 1985. Projection of the digit and wrist area of precentral gyrus to the putamen: relation between topography and physiological properties of neurons in the putamen. Brain. Res. 339, 245-255.

McGeorge, A.J., & Faull, R.L.M. 1989. The organization of the projection from the cerebral cortex to the striatum in the rat. Neurosci. 29, 503-537.

Parent, A., Charara, A., & Pinault, D. 1995. Single striatofugal axons arborizing in both pallidal segments and in the substantia nigra in primates. Brain Res. 698(1), 280-284.

Perreault, M.L., Hasbi, A., O'Dowd, B.F., & George, S.R. 2011. The dopamine D1–D2 receptor heteromer in striatal medium spiny neurons: evidence for a third distinct neuronal pathway in basal ganglia. Front. in Neuroanat. 5.

Polikov, V.S., Block, M.L., Fellous, J.M., Hong, J.S., & Reichert, W.M. 2006. In vitro model of glial scarring around neuroelectrodes chronically implanted in the CNS. Biomat. 27(31), 5368-5376.

Preibisch S., Saalfeld S., & Tomancak P. 2009. Globally optimal stitching of tiled 3D microscopic image acquisitions. Bioinformatics. 25(11), 1463-1465.

Reig, R., & Silberberg, G. 2014. Multisensory integration in the mouse striatum. Neuron. 83(5), 1200-1212.

Rothblat D.S., & Schneider J.S., 1995. Alterations in pallidal neuronal responses to peripheral sensory and striatal stimulation in symptomatic and recovered parkinsonian cats. Brain Res. 705(1), 1-14.

Tai, A.X., & Kromer, L.F. 2014. Corticofugal projections from medial primary somatosensory cortex avoid EphA7-expressing neurons in striatum and thalamus. Neurosci. 274, 409-18.

Thévenaz, P., Ruttimann, U.E, & Unser, M. 1998. A Pyramid Approach to Subpixel Registration Based on Intensity. IEEE Transactions on Image Processing. 7(1), 27-41.

Wall, N.R., De La Parra, M., Callaway, E.M., & Kreitzer, A.C. 2013. Differential innervation of direct-and indirect-pathway striatal projection neurons. Neuron. 79(2), 347-360.

West, M.O., Carelli, R.M., Cohen, S.M., Gardner, J.P., Pomerantz, M., Chapin, J.K., & Woodward, D.J. 1990. A region in the dorsolateral striatum of the rat exhibiting

single unit correlations with specific locomotor limb movements. J. Neurophysiol. 64, 690-703.

White, E.L., & DeAmicis, R.A. 1977. Afferent and efferent projections of the region in mouse SmL cortex which contains the posteromedial barrel subfield. J. Comp. Neurol. 175(4), 455-481.

Wilson, C.J., & Groves, P.M., 1980. Fine structure and synaptic connections of the common spiny neuron of the rat neostriatum: a study employing intracellular injection of horseradish peroxidase. J. Comp. Neurol. 194(3), 599-615.

Wu, Y., Richard, S., & Parent, A. 2000. The organization of the striatal output system: a single-cell juxtacellular labeling study in the rat. Neurosci Res. 38(1), 49-62.

Figures

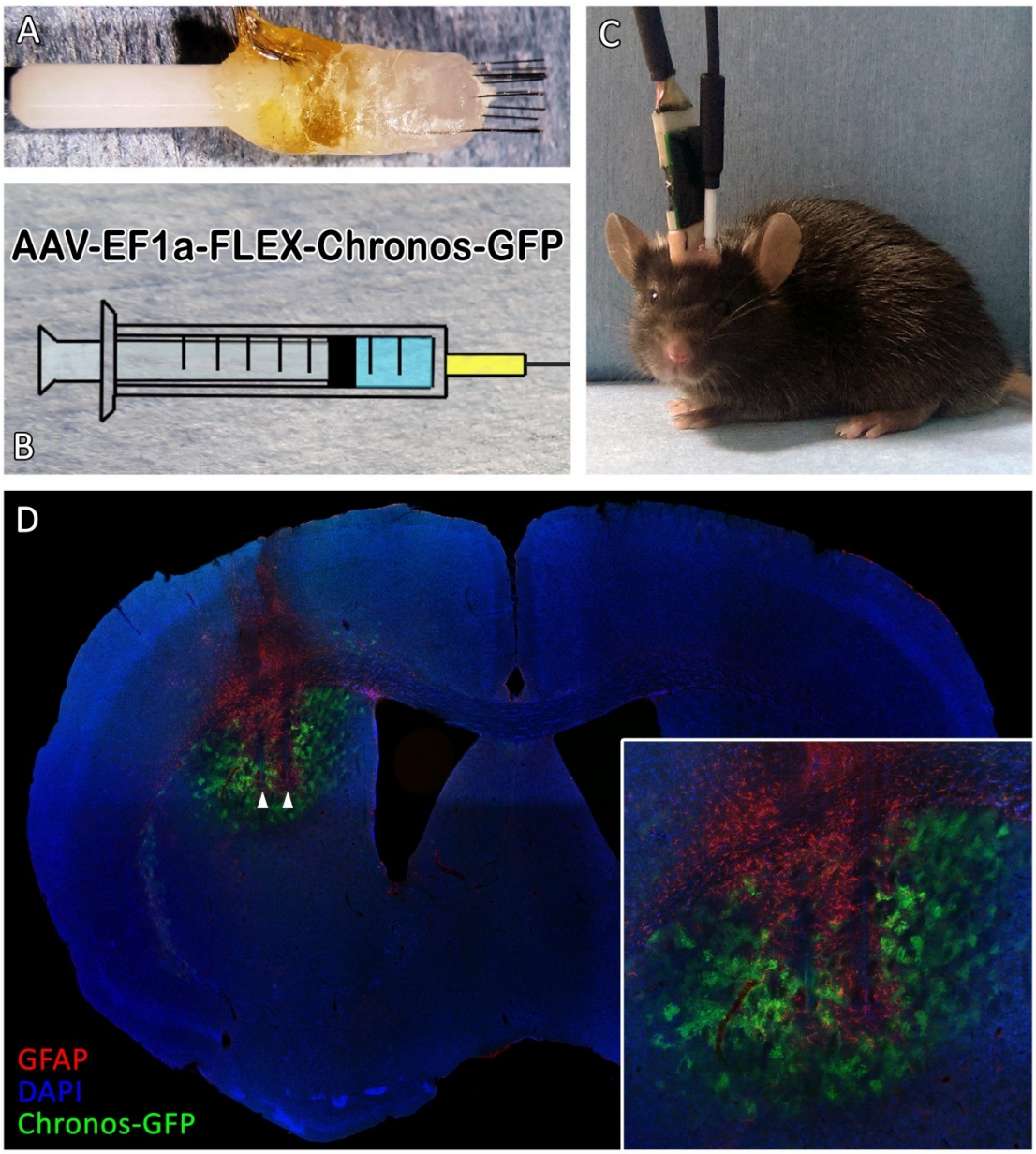

Figure 1. **A** Custom 15 microwire array with integrated optical fiber implanted in the dorsolateral striatum. **B** Representation of AAV-EF1a-FLEX-Chronos-GFP injected in the dorsolateral striatum for optogenetic identification. **C** Post surgery mouse connected to the electrophysiological recording harness and optical stimulation fiber simultaneously. **D** Example histological coronal slice from a Cre animal showing Chronos-GFP in green and GFAP in red on a DAPI counterstain. Wire tracks can be tracked to their tips within the expression of the virus using upregulated astrocytes (GFAP) along the wire tracks.

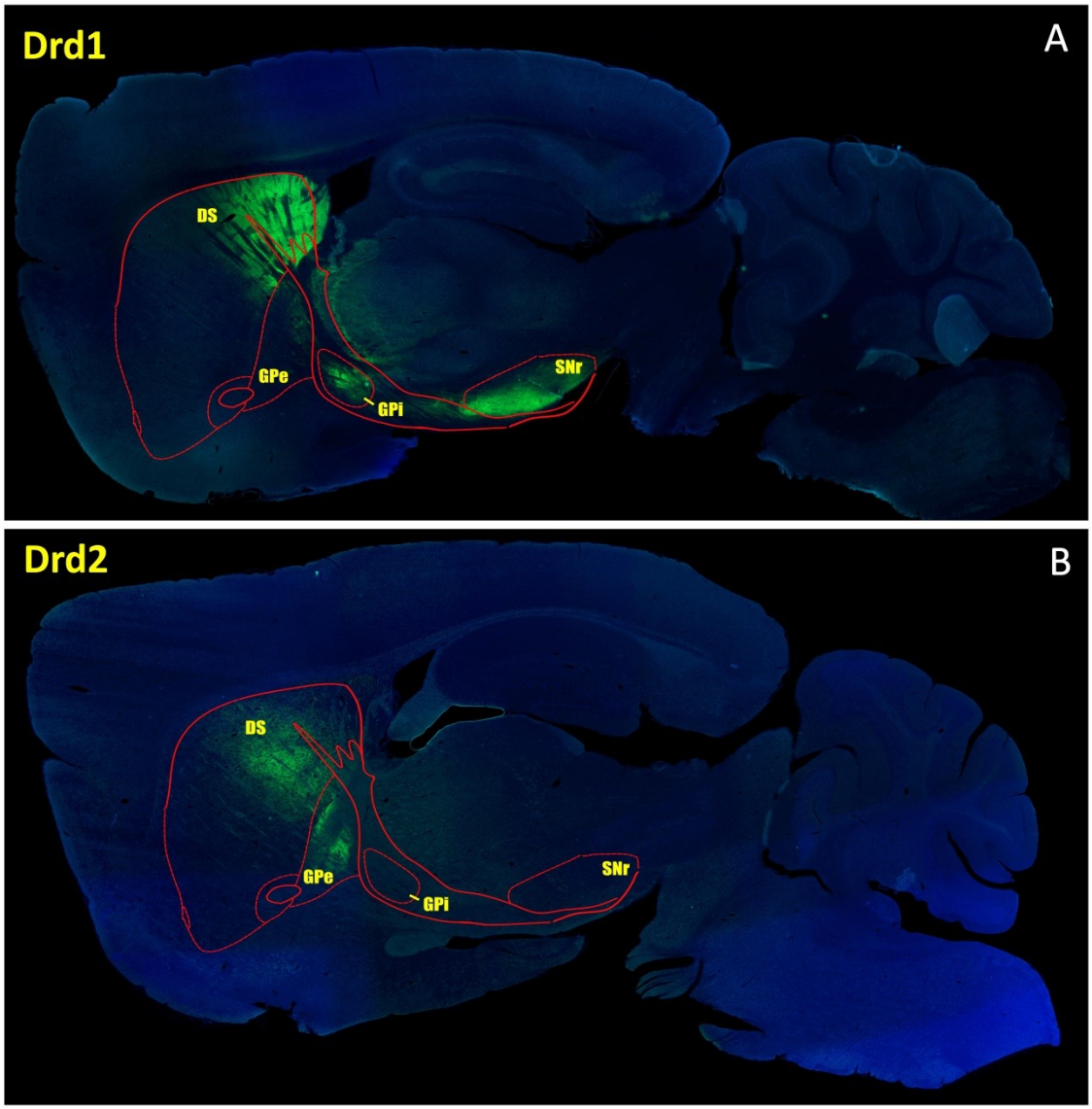

Figure 2. **A** Representative sagittal slice showing Chronos-GFP expression in the direct pathway of a Drd1-Cre mouse. **B** Representative sagittal slice showing Chronos-GFP expression in the indirect pathway of a Drd2-Cre mouse.

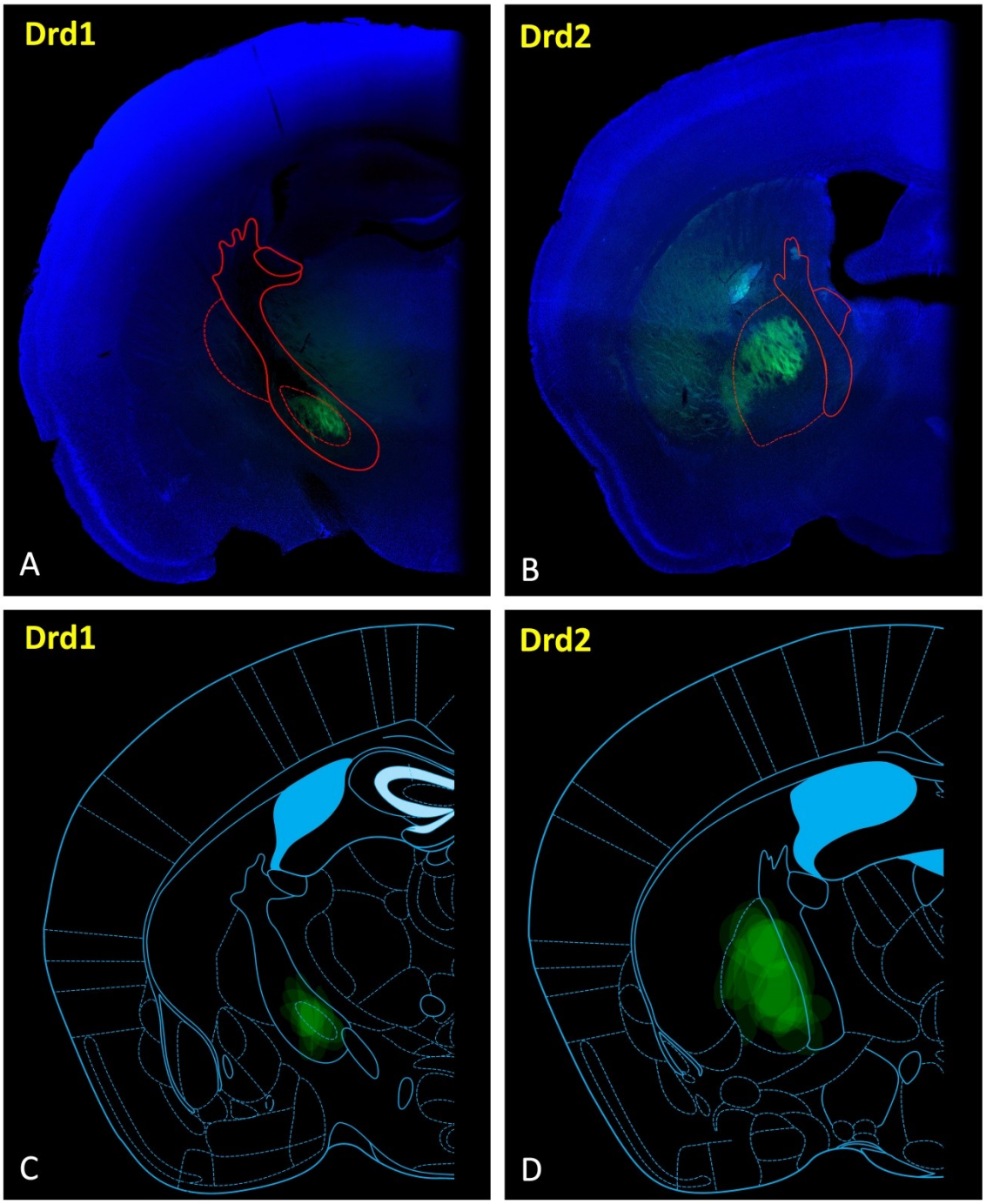

Figure 3. **A** Representative coronal slice showing Chronos-GFP expressing axon terminals in the GPi of an experimental Drd1-Cre mouse. **B** Representative coronal slice showing Chronos-GFP expressing axon terminals in the GPe of an experimental Drd2-Cre mouse. **C** Reconstruction of Chronos-GFP expressing axon terminals in the GPi of all experimental Drd1-Cre mice. **B** Reconstruction of Chronos-GFP expressing axon terminals in the GPe of all experimental Drd2-Cre mice.

Figure 4. **A** Summary of all 180 wires implanted into experimental animals. **B** Summary of all wild type neurons, not identified by optogenetic stimulation. **C** Summary of all neurons identified as Drd1 expressing MSNs of the direct pathway. **D** Summary of all neurons identified as Drd2 expressing MSNs of the indirect pathway.

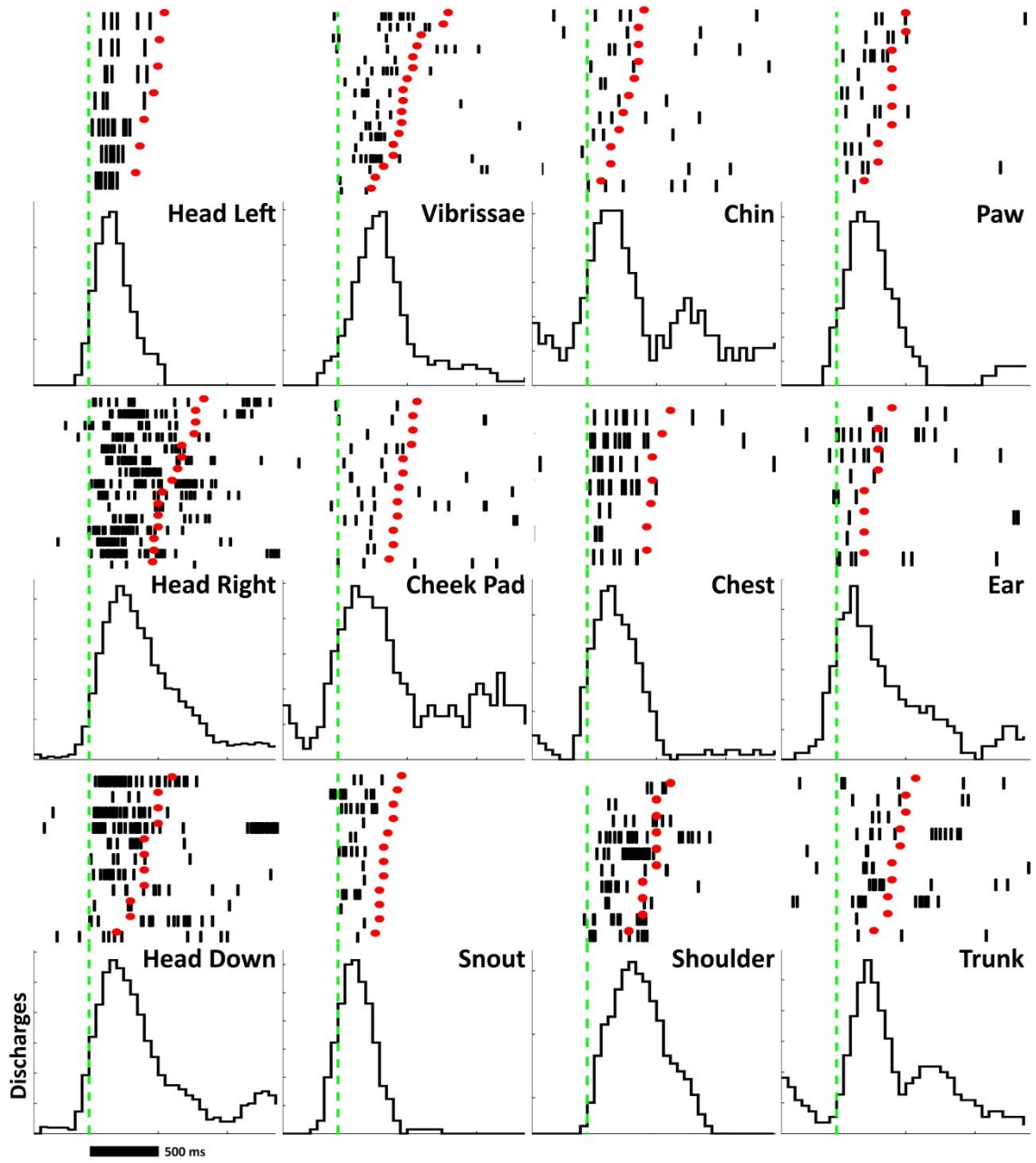

Figure 5. Example Raster-PETHs for each body part stimulated in this study from 12 unique type IIb neurons. Each row in the rasters contains 1 stimulation trial. Onset of stimulation is aligned to the green dashed line and offset of stimulation is marked with a red dot. Vertical ticks represent action potentials. The PETHs show a 5 point moving average of action potentials in 50ms bins.

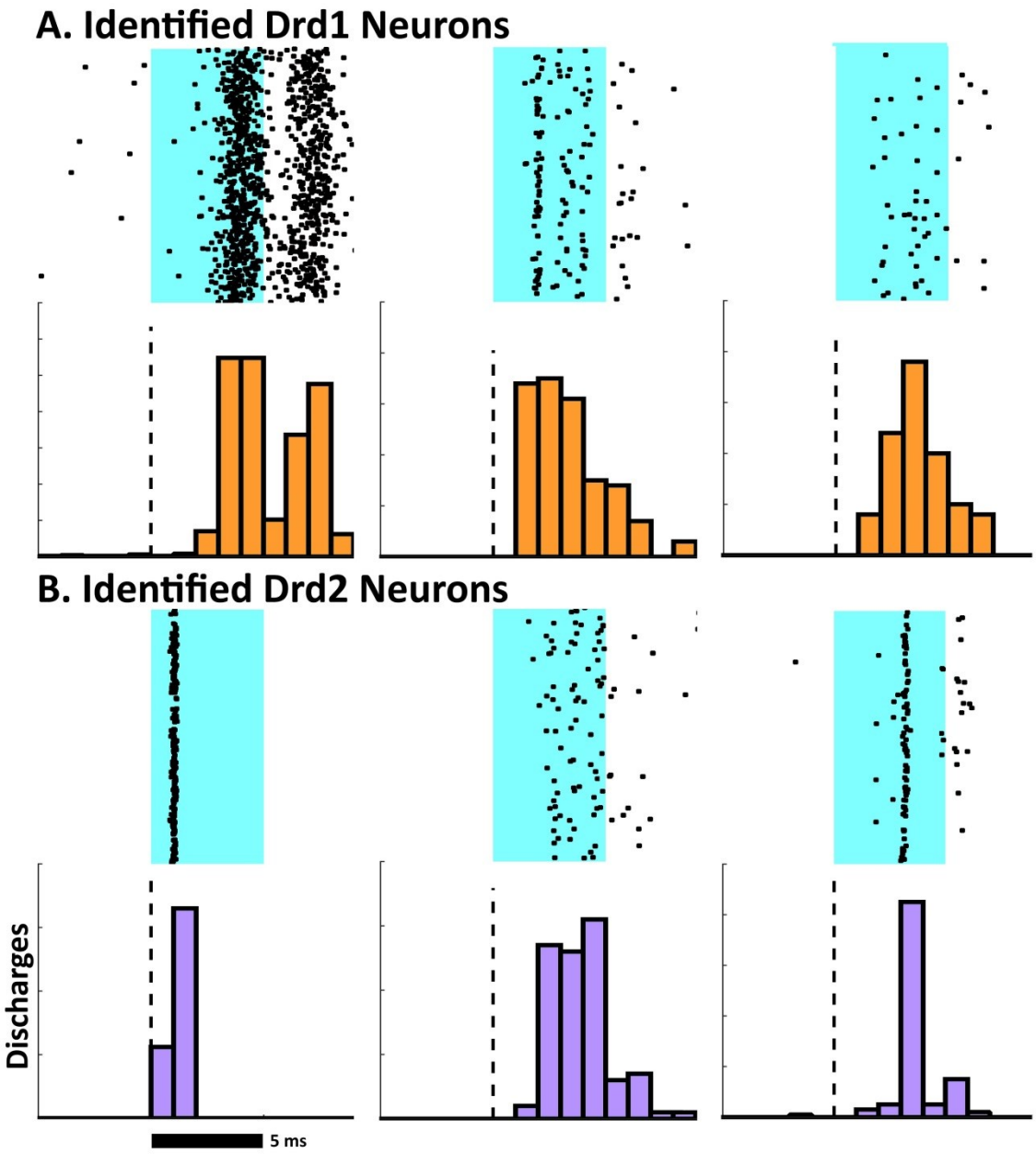

Figure 6. **A** Example Raster-PETHs from 3 unique optogenetically identified Drd1 neurons. **B** Example Raster-PETHs from 3 unique optogenetically identified Drd2 neurons. Each row in the rasters contains 1 light stimulation trial. Onset of stimulation is aligned to the dashed line and lasts for the duration of the cyan patch (5ms). Black dots represent action potentials. The PETHs show summation of action potentials in 1ms bins.

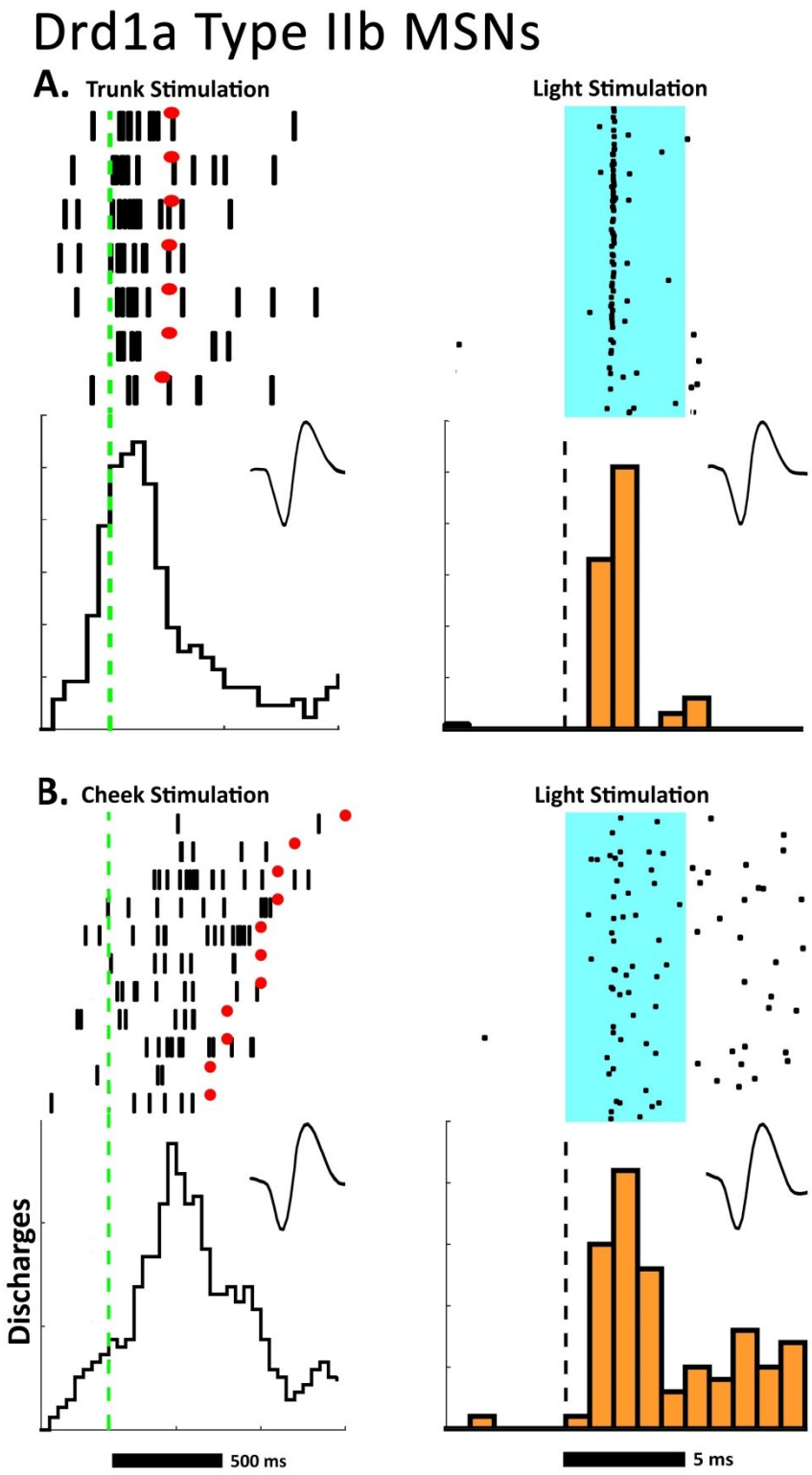

Figure 7. **A** Example Raster-PETHs from 1 optogenetically identified Drd1 type IIb neuron with firing related to trunk stimulation. **B** Example Raster-PETHs from 1 optogenetically identified Drd1 type IIb neuron with firing related to Cheek stimulation. All aspects of the Raster-PETHs are identical to the previous figures.

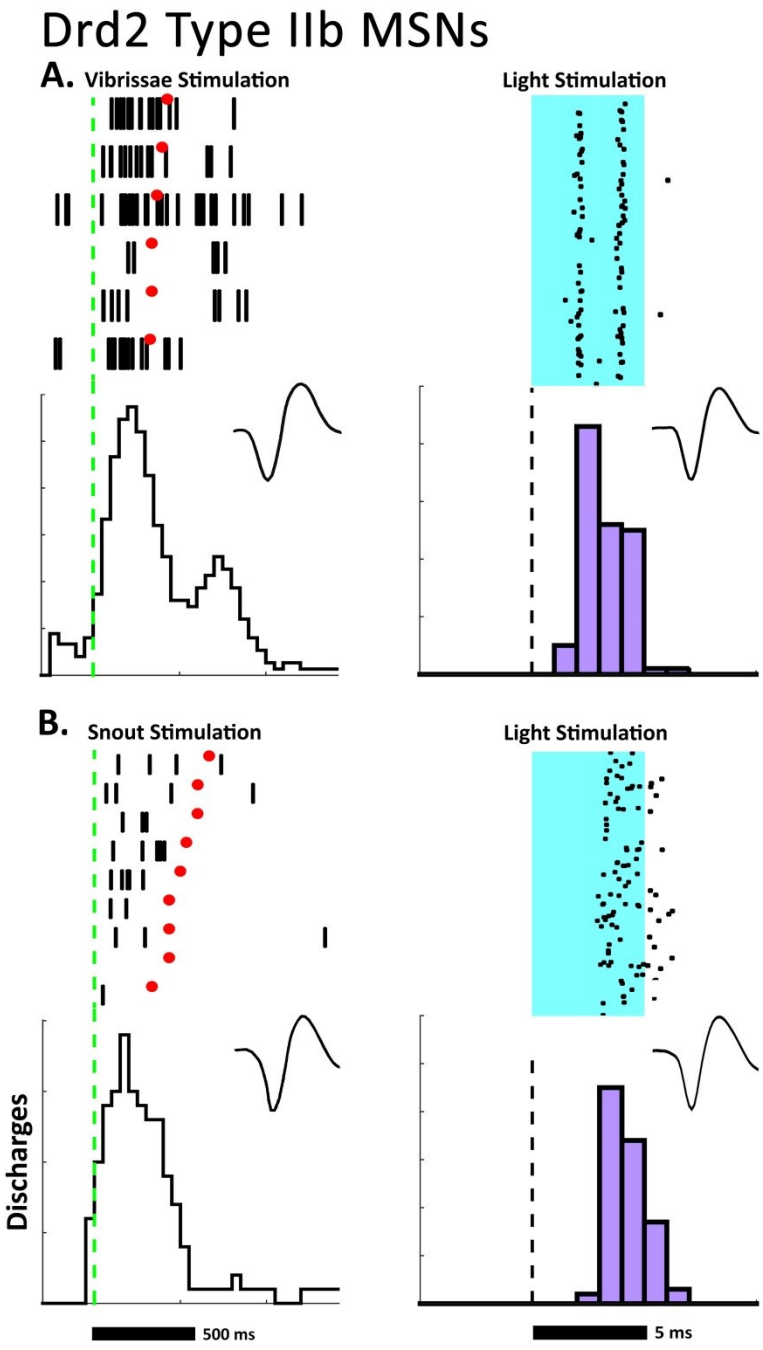

Figure 8. **A** Example Raster-PETHs from 1 optogenetically identified Drd2 type IIb neuron with firing related to vibrissea stimulation. **B** Example Raster-PETHs from 1 optogenetically identified Drd2 type IIb neuron with firing related to snout stimulation. All aspects of the Raster-PETHs are identical to the previous figures.

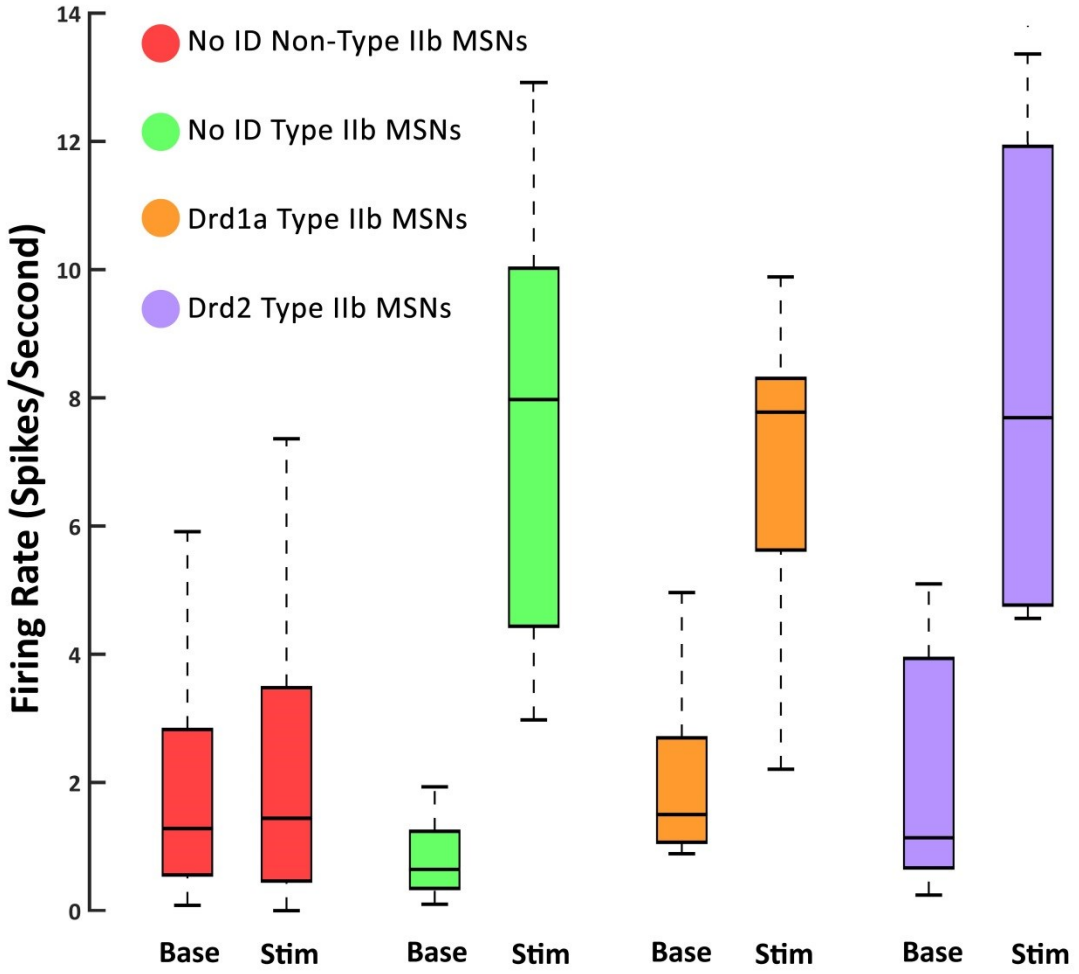

Figure 9. Average firing rates for all neurons during non-movement (**Base**) and body part stimulation (**Stim**). There was no significant difference in firing rate at baseline between any group, or between baseline and stimulation for non-type IIb MSNs. Firing rates during body part stimulation were also not significantly different for Drd1, Drd2, or unidentified type IIb MSNs. All type IIb MSNs fire similarly during stimulation of their related body part.

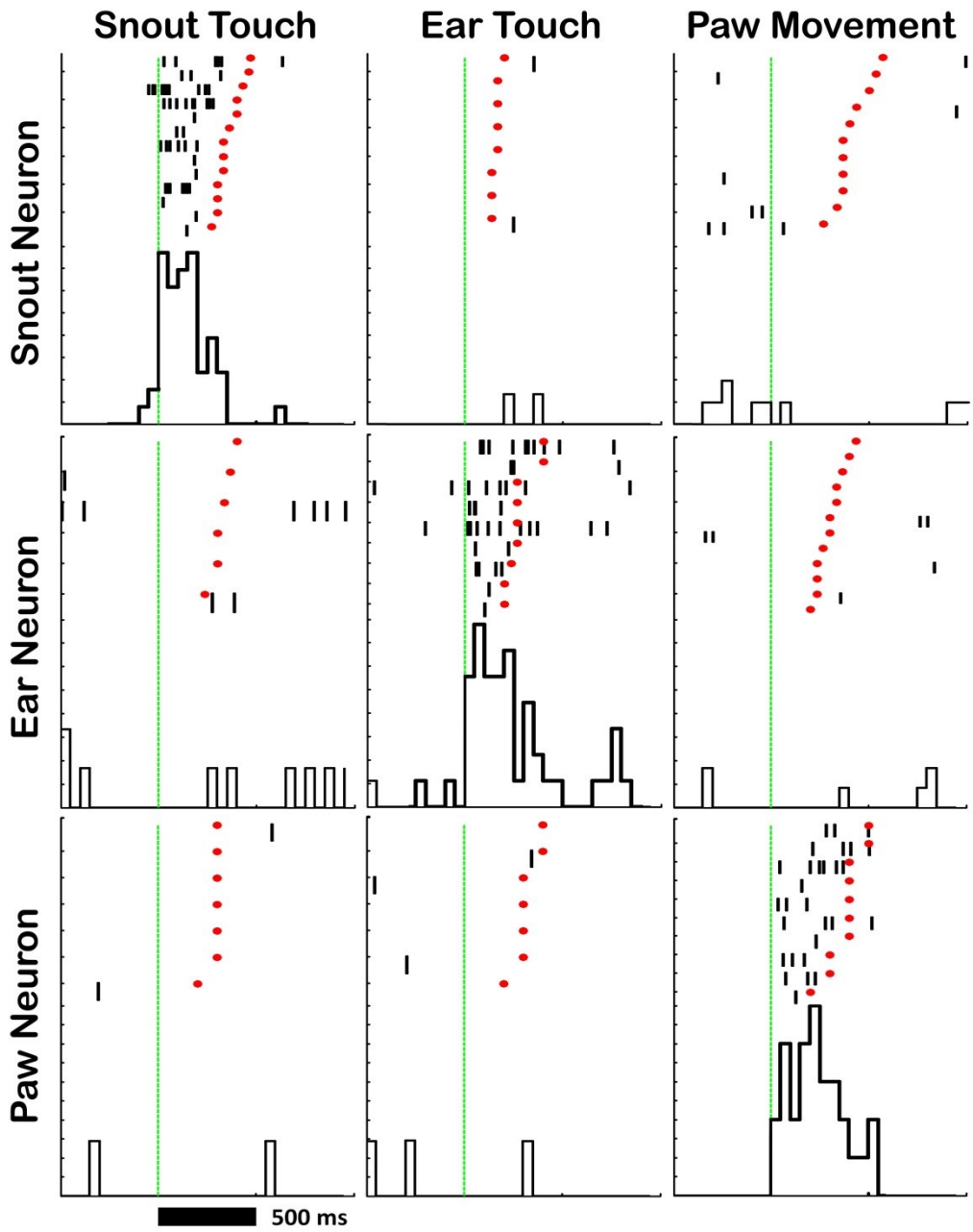

Figure 10. Example Raster-PETHs showing the selectivity of 3 different type IIb neurons. Each row has 3 Rater-PETHs from 1 neuron. Each column shows responses of the 3 different neurons to single body part stimulation. Notice how each neuron only fires during stimulation of its related body part, and not during stimulation of separate body parts. All aspects of the Raster-PETHs are identical to the previous figures.

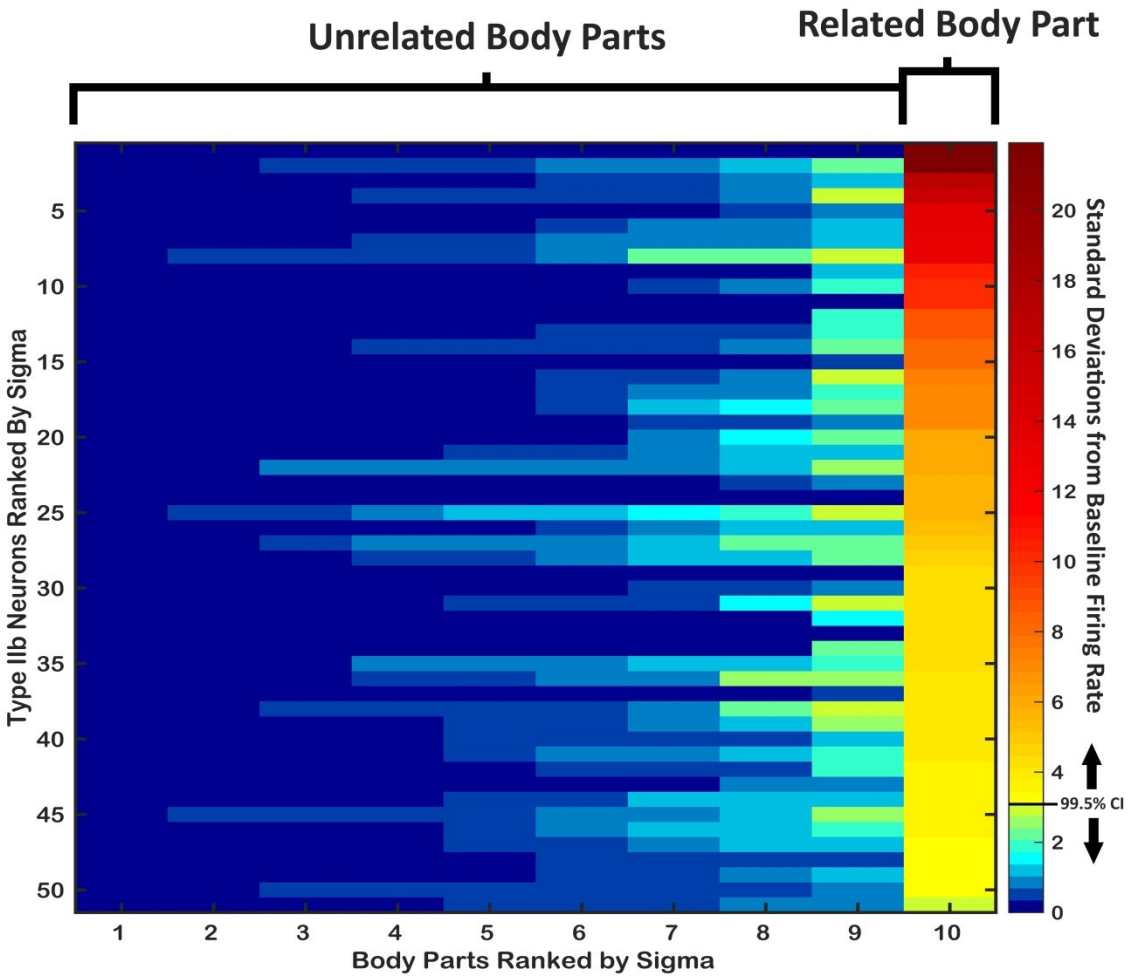

Figure 11. Heat map showing the extent of selectivity for all type IIb neurons in the study. Each row represents a single neuron and each column represents a body part. Firing rate during stimulation is converted to sigma (standard deviations from baseline firing rate) and coded in color. Each neuron's correlated body part is aligned to the right column, while each unrelated body part is shown in the remaining 9 columns, sorted from least to most firing during stimulation. All type IIb neurons fire highly selectively during stimulation of their correlated body part, and fire within the 99.5% confidence interval for baseline during all other body part stimulations.

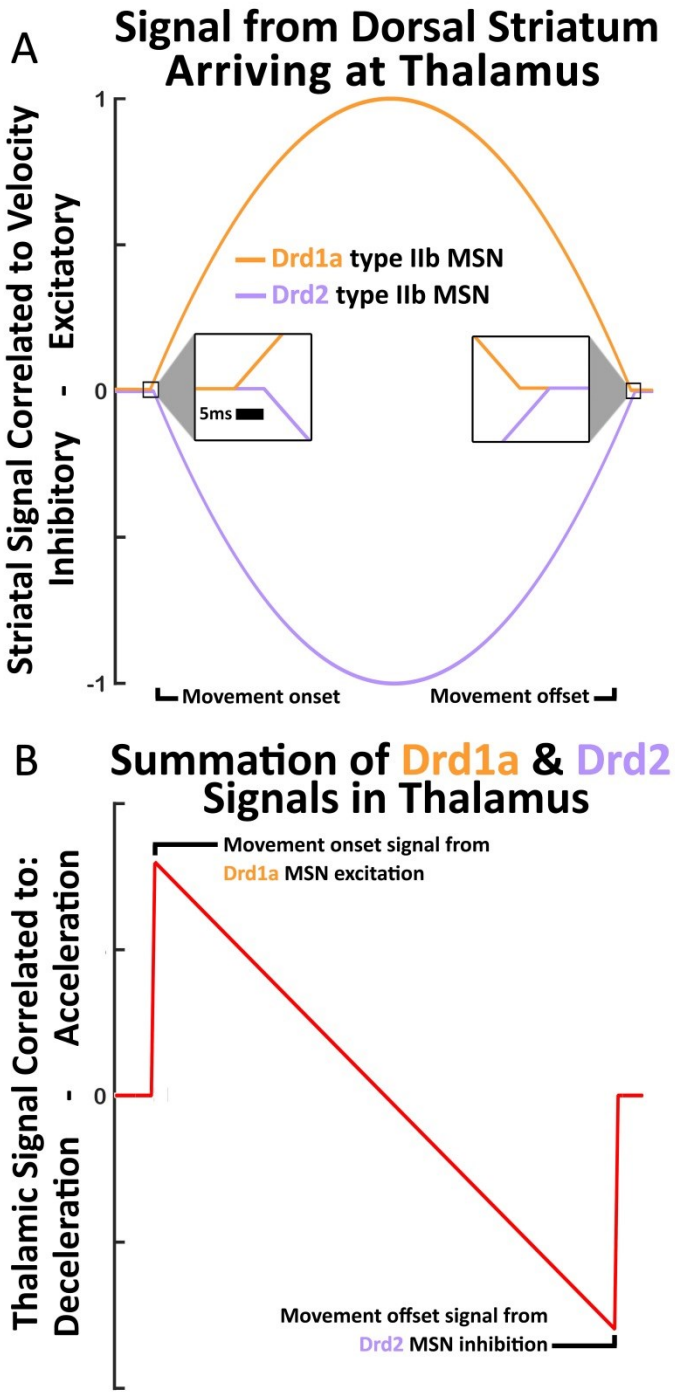

Figure 12. **A** Theoretical signals correlated to velocity from Drd1 and Drd2 neurons arriving at thalamus. Drd1 signals are excitatory and arrive first, while Drd2 signals are inhibitory and arrive lagged by ~15ms. **B** The summation of these signals in thalamus produces a unique pattern that carries new information. It contains a start signal from Drd1 excitation arriving alone, then a measure of change in velocity (acceleration), followed by a stop signal from Drd2 inhibition arriving alone.